AN ABSTRACT OF THE THESIS OF

Michael P. Summers for the degree of Master of Science in Mechanical Engineering
presented on September 5, 2013

Title: The Dynamic Shear Moduli of Blubber for Selected Large Whale Species

Abstract approved:

_____

John P. Parmigiani

Whale blubber is the insular tissue layer located between the dermis and the superficial fascia layer which sheathes the whale's musculature. It is made up of a lipid matrix ramified with strong, structural collagen and elastic fiber bundles, but little is known of its mechanical properties. Knowing these properties adds to the general knowledge of blubber and research that focuses on its physical response. Specifically, two current fields of research would gain from measurements of the complex dynamic shear modulus (G*=G'+iG"), a viscoelastic mechanical property, of blubber. The dynamic shear moduli G' and G" represent the elastic energy storage and the viscous energy dissipation, respectively. The first is drag reducing, compliant coatings, which seek to minimize the sonar signature and energy loss of submersibles. The second is subdermally attached satellite tracking tags that are remotely deployed into the dorsal region of large whales near the dorsal fin. The tags are used for

defining whale migration patterns and behaviors to help reduce potentially harmful human interactions. In this study, the dynamic shear moduli were measured at different depths and oscillating frequencies (0.31-25Hz, rotational rheometer) for blubber samples taken from a humpback whale, sperm whale, and two gray whales. A semi-quantitative staining assay was also performed to determine relative changes in normalized collagen and normalized non-collagen proteins with depth. For all four whales, G' and G" were plotted for each sample against a log scale of oscillating frequency. In all cases G' and G" were fit with a linear and 3rd order polynomial trend line, respectively. For the vast majority, R^2 was higher than 0.960. In some cases it dropped as low as 0.870. The G', G", and G"/G' data points for 0.31Hz, 3.1Hz, and 25Hz were plotted against sample coin depth in the blubber. Polynomials were traced through these data sets to characterize the depth profiles of these properties at these three separate oscillating frequencies. Depth profiles were also created for the measured collagen and non-collagen protein content. In conclusion, the results showed that different whale species may have distinctly different depth profiles of G', G", collagen protein, and non-collagen protein, but also show a similarity in the orders of magnitude of these metrics. A potential correlation exists between the ratios of non-collagen/collagen protein and G"/G'. However, an obvious direct relation could not be found between the moduli or the protein types.

The Dynamic Shear Moduli of Blubber for Selected Large Whale Species

by
Michael P. Summers

A THESIS

submitted to

Oregon State University

in partial fulfillment of
the requirements of the
degree of

Master of Science

Presented September 5, 2013
Commencement June 2014

Master of Science thesis of Michael P. Summers presented on September 5, 2013.

APPROVED:

Major Professor, representing Mechanical Engineering

Head of the School of Mechanical, Industrial, and Manufacturing Engineering

Dean of the Graduate School

I understand that my thesis will become part of the permanent collection of Oregon State University libraries. My signature below authorizes release of my thesis to any reader upon request.

Michael P. Summers, Author

ACKNOWLEDGEMENTS

I would like to express my sincere gratitude to my advisor Dr. John Parmigiani. The completion of my degree would not have been possible without his support, enthusiasm, and the opportunity he provided me.

I would also like to thank my committee members Dr. William Warnes and Dr. Skip Rochefort for their input and assistance throughout my graduate research.

My thanks also go out to Dr. Bruce Mate, Dr. Deborah Duffield, Dr. Barbara Taylor, Jim Rice, Peter Oliver, Rachel Feigner, Jonathan Holst, and Meghan Atkinson for working with me, supporting me, and acting as excellent resources during my research.

Finally, I must thank my friends, family, and fellow graduate students for their ongoing encouragement and motivation. They helped make graduate school a fulfilling and enjoyable experience.

TABLE OF CONTENTS

LIST OF FIGURES (Continued)

Figure Page

LIST OF FIGURES (Continued)

Figure Page

LIST OF FIGURES (Continued)

Figure Page

LIST OF TABLES

Table Page

The Dynamic Shear Moduli of Blubber for Selected Large Whale Species

1 Introduction

There has been very little published on the mechanical properties of whale blubber. A further investigation of these properties not only adds to the general knowledge of blubber, but also benefits those that use them. Located below the dermas, blubber is an insular tissue constructed of a lipid matrix cross-weaved with strong, structural collagen and elastic fiber bundles. The blubber transitions into the superficial fascia layer, a loose connective tissue, which sheaths the muscle surrounding the whale. [1] Blubber is expected to behave viscoelastically because it is a soft tissue. [2] The complex dynamic shear modulus G*=G'+iG" is a viscoelastic property commonly used in defining soft tissues. It is comprised of both an elastic energy storage term (G') and a viscous energy dissipation term (G"), which are known as the dynamic shear moduli. Apart from adding to the morphology of whale blubber, these properties can currently be used for the improvement of certain whale tracking tag designs. The tags that would gain from these measurements deploy remotely and anchor subdermally in the body of large whales, near the dorsal fin. Once attached, they transmit a radio signal to a monitoring satellite. Knowing the migratory and behavioral patterns of whales allows for the adjustment of human activities to help in the recovery of endangered species. [3] It also furthers the ecological knowledge of the ocean.

Only two papers were found that studied the mechanical properties of blubber. In 1987, Orton and Brodie measured the tensile modulus of the ventral groove of a fin whale to better understand their locomotion and engulfing mechanics during lunge feeding. [4] Fitzgerald and Fitzgerald, in 1995, published the only article that currently relates to the viscoelastic properties of blubber. They measured the complex dynamic shear compliance ($J^*=1/G^*$) of pilot whale blubber. [5] Measurements were from a single whale soon after its death. The results showed that the tissue's complex dynamic shear compliance decreased over time until it reached a fully necrotic state, where the compliance stabilized. Given this data, an extrapolation was made to define the live tissue compliance. These values were compared with candidate materials for drag reduction compliant coatings. The application of these coatings is to reduce the energy loss due to drag on submersibles as well as reducing their sonar profile. Though the dynamic shear moduli can be calculated from this data, it only represents a value for a single species at a single depth beneath the dermis.

This study measured the dynamic shear moduli of blubber at different depths beneath the dermis. Samples were taken from deceased, stranded whales: a humpback whale, sperm whale, and two gray whales. The results of these measurements were then compared with the relative amounts of collagen and non-collagen proteins, at these various depths. The following sections cover the sample preparation and test protocols, the results obtained from these methods, a discussion of how these values compare with one another and to the pilot whale study, and lastly, concluding remarks and recommendations for further research.

2 Methods

2.1 Dynamic Shear Moduli

Coin shaped tissue samples were created for rheometric analysis. A block of blubber was first excised from a stranded whale and then frozen. Before rheometric analysis, this block was thawed and then cored using a rotating sharpened tube attached to a handheld drill. This created tissue columns within the block that were still attached to the superficial fascia layer at the base of the block. A commercial deli slicer was then used to cut the block numerous times. This converted the columns into coin-shaped tissue samples that could be loaded into the rheometer. Coins were chosen at specific depths for testing, based on a reasonable distribution of the full depth of the tissue. This reduced the number of tests required to define a depth profile of the dynamic shear moduli throughout the thickness of the whale's blubber.

The thickness, diameter, circularity, and depth of each sample coin were measured using an optical microscope that was outfitted with a digital coordinate display. For the thickness, each coin was placed on its edge between two aluminum blocks, and the distance between the edges of the blocks was measured. For the diameter and circularity, each coin was placed flat, on a plate, and oriented so that it's shortest and longest axes were measured. These two measurements were averaged for the diametric average, and subtracted for the diametric difference (a perfect circle would be estimated by a diametric difference of zero). Lastly, the depth of a coin is

reported as a percentage of the full depth of the blubber. It is defined as the distance from the dermis to the center of the coin divided by the full thickness of the blubber.

A rotational rheometer (AR2000ex, TA Instruments) was used to measure the dynamic shear moduli (G' and G"). Two metal platens press a coin sample with a constant normal force and induce dynamic shear with rotational oscillations (Figure 1). One plate actuates the oscillations at a set frequency and percent strain on the sample, while the other plate measures the stress/strain response. The peaks of the actuation stress curve and the response strain curve, along with the phase shift between them, that defines the dynamic shear moduli G' and G". Sandpaper (400grit) was glued to both of the platens to prevent the coin sample from slipping at higher frequencies. The measurement resolution, which is discussed later in this document, is defined by the repeatability of testing soft tissues. The high accuracy of the rheometer minimally contributes to this measurement variability.

Figure 1: A blubber sample coin loaded in the AR2000ex rotational rheometer to measure the dynamic shear moduli G' and G".

Three types of tests were performed using the rheometer: 1) frequency sweep test, 2) repeat frequency sweep test, and 3) strain sweep test. All of which were performed at room temperature (19-22°C). The frequency sweep test was conducted to measure the dynamic shear moduli over a range of oscillating frequencies. Nominally, each coin sample was placed under a constant normal force of 40N, and then oscillated with 1% strain over a frequency range 0.31Hz-25Hz (21 equally spaced frequencies). The repeat frequency sweep test was performed on a sub-selection of coins, to determine the measurement repeatability. It was an identical frequency sweep test that was repeated immediately following its initial test. The strain sweep test was used to determine if 1% strain was damaging the tissue samples during the frequency sweep tests. Following the initial frequency sweep test a sub-selection of coins (alternate to those used in the repeat frequency sweep test) were strain swept. The samples were placed under a 40N normal force, while oscillated at a set frequency of 1Hz with a 0.1-2% strain range. This test was then repeated at a frequency of 10Hz. Over the course of the entire preparation process and these three test series testing process the sample coins remained in sealed plastic bags categorized by their selected depth (anywhere from 6-10 samples per bag). This was done to reduce desiccation and oxidation. The testing order was randomized by sealed bag (depth), but sequential, by column, within a bag.

2.2 Collagen/Non-Collagen Protein

The relative amounts of collagen and non-collagen protein were measured using a semi-quantitative staining assay protocol; by Chondrex, Inc. [6] Slight adjustments

were made to this protocol due to the overly thick tissue sections that were used. A commercial deli slicer cut thin cross-sections from the blocks of blubber that were used to make the sample coins, and then frozen. On the day of testing, these samples were thawed and placed in a 9:1 fixative solution of phosphate buffered saline (PBS, 6mmol/L Na2HP04; 1.67mmol/L NaH2P04; 137mmol/L NaCl; pH=7.4), which is isotonic for mammalian tissues, and a formaldehyde solution called formalin (Mallinckrodt Baker Chemicals, VWR International). After the tissue sections from each whale were fixed (30 minutes), the sections were first rinsed with PBS and then with water. Each section was then submerged in its own 25mL tray of Sirius Red / Fast Green stain (Chondrex ID#90461) for 20 minutes (flipped after 10min). During this time, the sections were agitated on a revolving platform and lightly by hand to maintain adequate coverage. The sections were then de-stained in a water bath that was frequently refreshed, over the course of an hour. At this point, the diffusion of stain from the tissue into the water bath was sufficiently slow. The sections were removed from the bath and a razor blade was used to cut three, full-length columns from each section. These columns were then cut into squares, and measured with calipers. Each square was placed in its own container filled with 17mL of stain extraction buffer (Chondrex ID90462) and placed on the revolving platform. After three days the squares were removed, the containers were randomized, and their protein content was analyzed. To perform this analysis ~1mL of fluid was taken from a container and placed in a cuvette, which was loaded into the spectrophotometer. The absorbency of both 540nm and 605nm wave lengths were measured and used to

calculate the amount of collagen and non-collagen protein (μg/section) for each container. However, the Chondrex protocol requires that the tissue sections be 10-20μm thick. Though blubber has not been used with this protocol before, it is thought, by Chondrex, that stain will only penetrate 5-10μm. The sections cut in this study were ~1-3mm thick. Since the stain will only penetrate the surfaces of these sections the resulting protein concentrations were normalized with respect to the cross-sectional area of each square. This creates results that show the relative change in protein concentration rather than the absolute value. To increase the accuracy of this method, all tissue squares were cut on all sides so no edges contained stain. Two measurements were made on each container and averaged. The containers were re-randomized between each measurement.

3 Results

3.1 Dynamic Shear Moduli

3.1.1 General Observations

There were certain regularities that were shared by all of the whales. During preparation, the coin samples nearer to the dermis felt stiffer to the touch than those deeper in the tissue. Also, these deeper samples became less opaque, and a cross hatch of fiber bundles was revealed. During testing, the peak variability in applied normal load and percent strain across all of the sample coins was 1N and 0.13%. However, the variability for the vast majority of the sample coins was <0.2N and <0.05% strain. For

all of the samples, the highest variability of percent strain occurred near 0.31Hz and 25Hz. Lastly, fluid was seen being slowly pressed out of all of the sample coins during testing.

3.1.2 Humpback Whale

A blubber sample was collected and prepared from a sub-adult humpback whale that was 8.23m long. It was stranded on Baker Beach (9.7km north of Florence, OR). The cause of death was unknown. The blubber was excised (83.3-89.5mm thick blubber layer) from its body approximately 1.08m behind the left lateral fin, and then frozen (Nov. 16th, 2012). On Dec. 12th, 2012 (26 days in storage) the block was thawed, prepared, and tested as described in the methods section. Six columns were cut into the block of blubber, all within a $0.3m^2$ area. Within these six columns, 33 sample coins, at various depths, were tested. The geometry of the tested coins was evaluated to see if their variability caused variability in the dynamic shear moduli measurements (Table 1). The variability of most of these values was expected, given the difficulty of cutting soft tissue. However, the maximum diametric difference (10.0mm) is abnormally high when considering its average (1.9mm) and the minimum (0.2mm). The four samples closest to the dermis are the cause of this. They are highly elliptical in shape (diametric differences >8mm). The rest of the samples had far more reasonable diametric differences (<2mm).

Table 1: The range of geometric values measured for the humpback whale sample coins.

Humpback Whale: Coin-Sample Geometries			
	Maximum	Average	Minimum
Thickness (mm)	3.5	3.0	2.6
Diametric Average (mm)	23.7	22.1	19.8
Diametric Difference (mm)	10.0	1.9	0.2

A representative sample coin was selected to show the typical moduli measurements for the humpback whale. Figure 2 plots G' and G" against the log scale of the oscillating frequency. The coin selected was taken from a 37.1% depth in the tissue. It was 3.2mm thick, had an average diameter of 22.7mm, and a diametric difference of 0.2mm. G' in this data set shows a positive linear trend and G" shows a 3rd order polynomial trend.

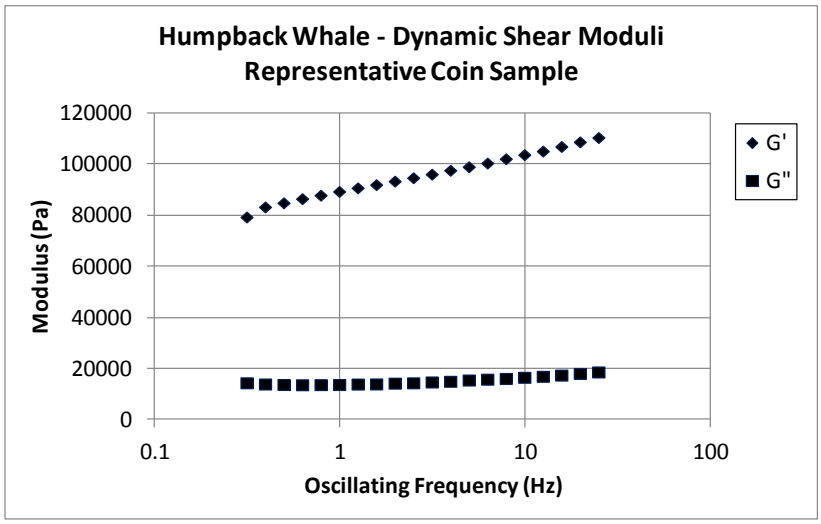

Figure 2: The data set of the representative sample coin for the humpback whale. It shows the value of G' and G" as it changes with the log scale of the oscillating frequency. A conservative estimate for the highest machine measurement error is1500Pa.

Trend lines were fit to the moduli of all of the sample coins. The coefficient of determination (R^2) of these trend lines were plotted as they varied with depth (Figure 3). Using a log scale for the oscillating frequency, the G' and G" were fit with a linear and 3rd order polynomial respectively. All of the fits showed high agreement with R^2

above 0.975. The vast majority were above R^2=0.990. A polynomial traced through the R^2 data points to define a general depth profile. From this, no large changes were seen (based on scaling).

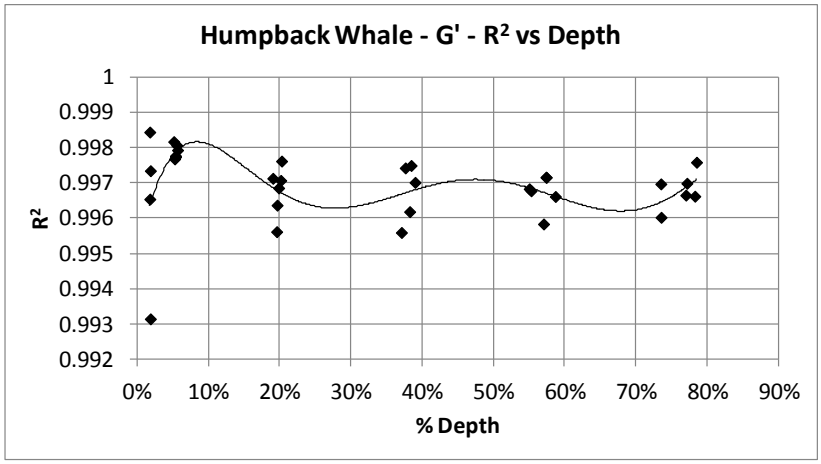

(a)

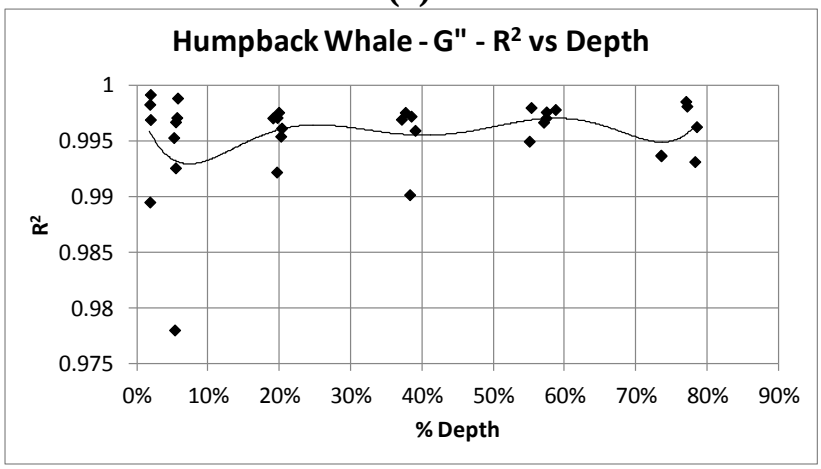

(b)

Figure 3: a) R^2 plotted against depth, for the trend lines of all of the sample coins in the humpback whale: a) G' – linear fit b) G" – 3rd order polynomial fit.

Figure 4 is a series of plots, each showing the general depth profile of a different rheometric property for the Humpback whale. In each plot, the 3.1Hz data points from all 33 sample coins are plotted against depth, and a polynomial traces the general depth profile through this data. In addition, polynomials are traced through the

25Hz and 0.31Hz data points. For clarity, the data points for these latter two data sets are not shown. The shapes of all three depth profiles are similar in each plot. For G' and G", the profiles show a general trend between ~22% and ~55% depth. The sections of the profiles that are shallower and deeper than this middle region show a different behavior. This may be due to a transition in tissue constituents as it gets closer to the dermis and the superficial fascia layer. This profile region separation is less distinct for the G"/G' plot, which shows a general increase with depth.

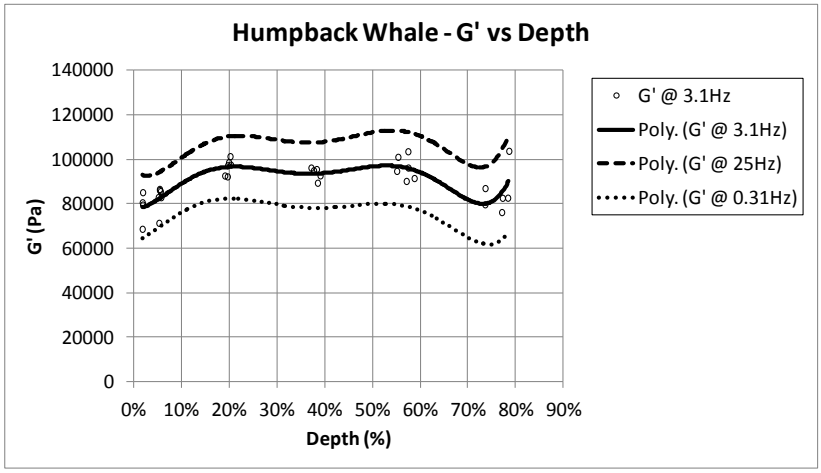

(a)

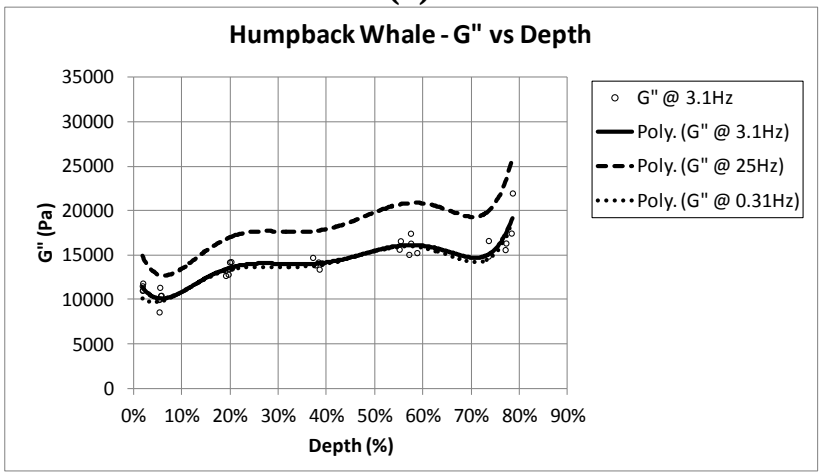

(b)

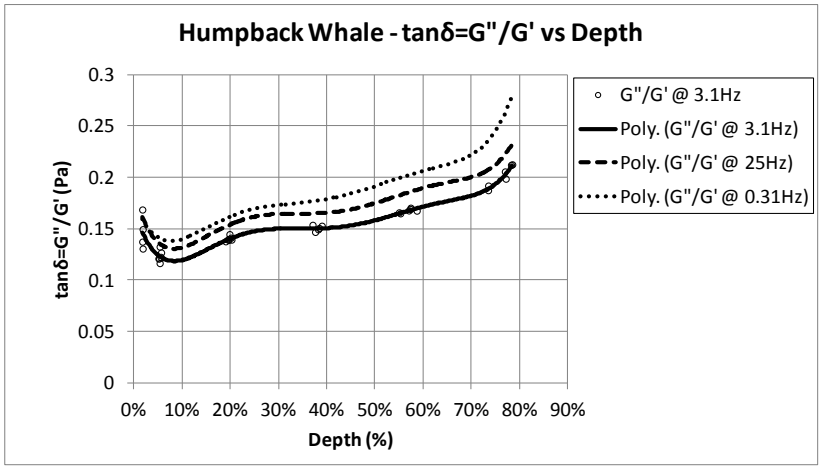

(c)

Figure 4: A series of plots that show rheometric properties as they vary with depth in the humpback whale. Displayed are the data points measured at 3.1Hz and depth profile traces through these data points and the data points of 25Hz and 0.31Hz: a) G' b) G" c) tanδ=G"/G'

3.1.3 Gray Whale #1

A blubber sample from an adult, male gray whale (12.87m long) was received from Dr. Deborah Duffield (Portland State University, Department of Biology). It was collected by the Northern Oregon/Southern Washington Marine Mammal Stranding Network. The stranding was just south of Bolstad Ave. access, Long Beach, WA, and the cause of death was suspected to be lymphoma with fungal infection. The sample block (84.9-88.5mm thick blubber layer) was excised from the mid-lateral right side of thorax. It was removed on March 10th, 2012, and frozen. In February 2013 (11 months in storage) the block was thawed, prepared, and tested as described in the methods section. Ten columns were cut into the block, all within a $0.3m^2$ area. Within these ten columns, 37 sample coins at various depths were tested.

The geometry of the tested coins was evaluated to see if their variability caused variability in the dynamic shear moduli measurements (Table 2). The variability of

these values was expected, given the difficulty of cutting soft tissue. There was no indication of any large geometric imbalances for this data set.

Table 2: The range of geometric values measured for the gray whale #1 sample coins.

Gray Whale #1: Coin-Sample Geometries			
	Maximum	Average	Minimum
Thickness (mm)	3.5	2.7	2.0
Diametric Average (mm)	21.6	20.7	19.5
Diametric Difference (mm)	4.1	1.0	0.02

A representative sample coin was selected to show the typical moduli measurements for gray whale #1. Figure 5 plots G' and G" against the log scale of the oscillating frequency. The coin selected was taken from a 35.3% depth in the tissue. It was 2.8mm thick, had an average diameter of 21.3mm, and a diametric difference of 0.1mm. G' in this data set shows a positive linear trend and G" shows a 3rd order polynomial trend.

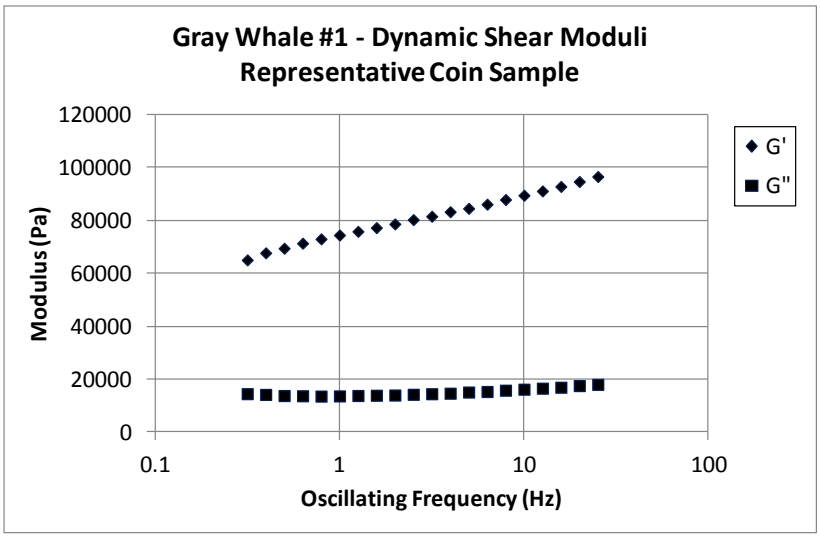

Figure 5: The data set of the representative sample coin for gray whale #1. It shows the value of G' and G" as it changes with the log scale of the oscillating frequency. A conservative estimate for the highest machine measurement error is1500Pa.

Trend lines were fit to the moduli of all of the sample coins for gray whale #1. The coefficient of determination (R^2) of these trend lines were plotted as they varied with depth (Figure 6). Using a log scale for the oscillating frequency, the G' and G" were fit with a linear and 3rd order polynomial respectively. All of the fits showed high agreement with R^2 above 0.965. The vast majority were above R^2=0.995. A polynomial traced through the R^2 data points to define a general depth profile. From this, no large changes were seen (based on scaling).

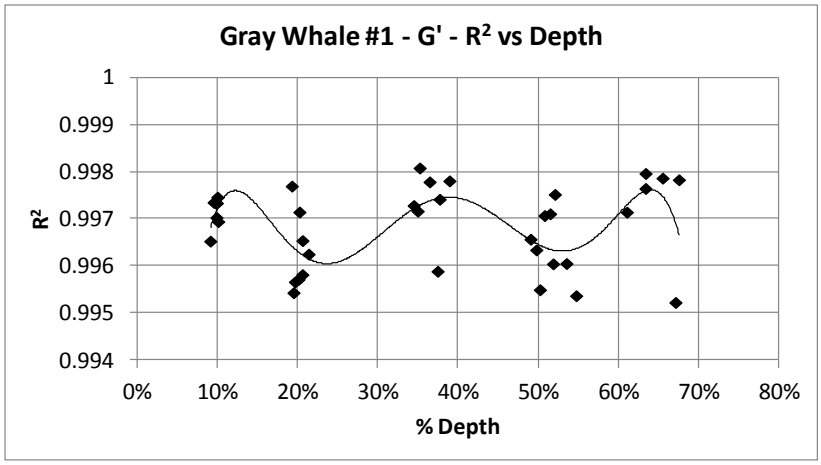

(a)

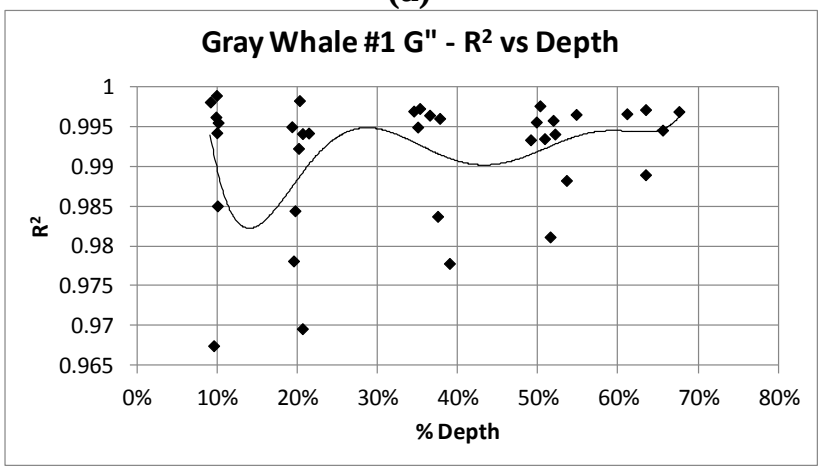

(b)

Figure 6: a) R^2 plotted against depth, for the trend lines of all of the sample coins in gray whale #1: a) G' – linear fit b) G" – 3rd order polynomial fit.

Figure 7 is a series of plots, each showing the general depth profile of a different rheometric property for gray whale #1. In each plot, the 3.1Hz data points from all 37 sample coins are plotted against depth, and a polynomial traces the general depth profile through this data. In addition, polynomials are traced through the 25Hz and 0.31Hz data points. For clarity, the data points for these latter two data sets are not shown. The shapes of all three depth profiles are similar in each plot. For G' and G", the profiles show a general linear trend between ~20% and ~58% depth. The sections of the profiles that are shallower and deeper than this middle region show a different behavior. This may be due to a transition in tissue constituents as it gets closer to the dermis and the superficial fascia layer. This profile region separation is less distinct for the G"/G' plot, which shows a slight increase with depth for the 0.31Hz data, but remains relatively constant for the 3.1Hz and 25Hz data.

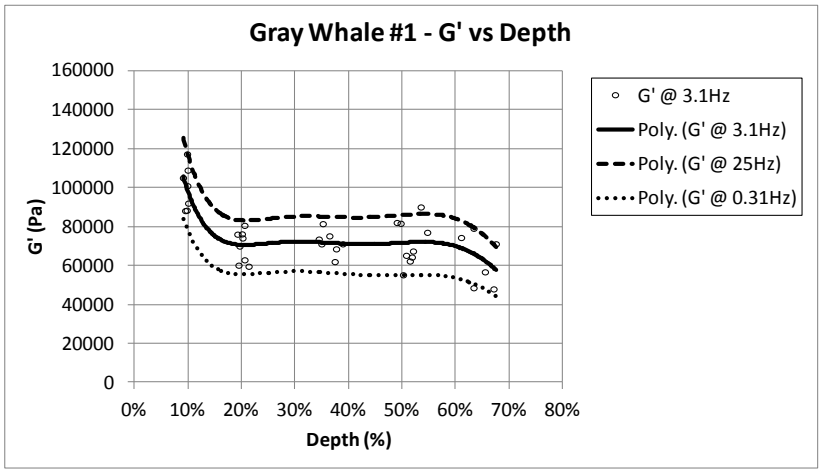

(a)

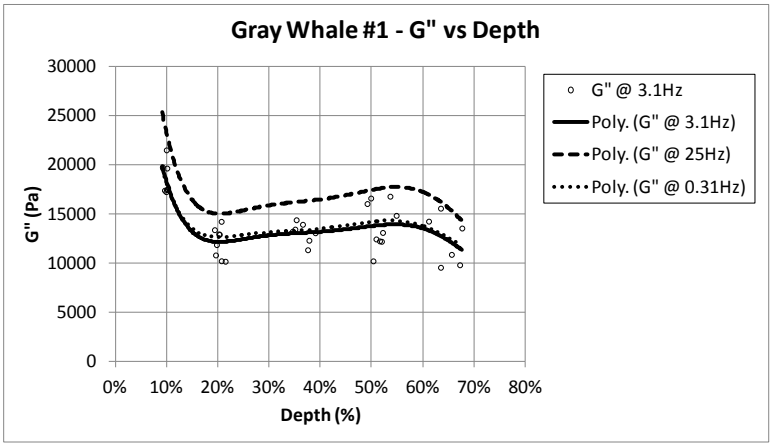

(b)

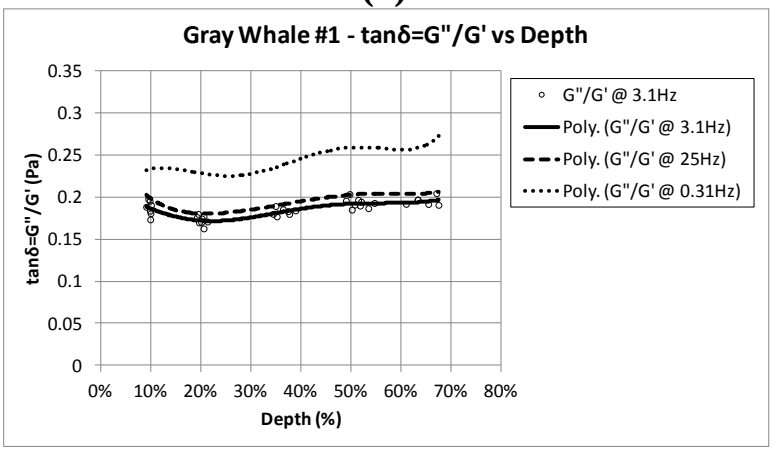

(c)

Figure 7: A series of plots that show rheometric properties as they vary with depth in gray whale #1. Displayed are the data points measured at 3.1Hz and depth profile traces through these data points and the data points of 25Hz and 0.31Hz: a) G' b) G" c) tanδ=G"/G'

3.1.4 Gray Whale #2

A blubber sample was collected and prepared from a sub-adult, female gray whale that was 12.12m long. It was stranded just south of Face Rock Wayside, Bandon, OR, and the cause of death was unknown. The sample block was excised (118.1-122.2mm thick blubber layer) just below the mid-body line on the lateral side, and in line with the dorsal fin. It was removed on December 27th, 2011, and frozen. In March 2013 (15 months in storage) the block was thawed, prepared, and tested as

described in the methods section. Ten columns were cut into the block, all within a $0.3m^2$ area. Within these ten columns, 58 sample coins, at various depths, were tested. The geometry of the tested coins was evaluated to see if their variability caused variability in the dynamic shear moduli measurements (Table 3). The variability of most of these values was expected, given the difficulty of cutting soft tissue. Though not a large imbalance most of the sample coins nearest to the dermis were more elliptical than the others.

Table 3: The range of geometric values measured for the gray whale #2 sample coins.

Gray Whale #2: Coin-Sample Geometries			
	Maximum	**Average**	**Minimum**
Thickness (mm)	4.5	3.1	2.1
Diametric Average (mm)	24.5	21.8	19.4
Diametric Difference (mm)	3.6	2.0	0.2

A representative sample coin was selected to show the typical moduli measurements for gray whale #2. Figure 8 plots G' and G" against the log scale of the oscillating frequency. The coin selected was taken from a 40.6% depth in the tissue. It was 3.1mm thick, had an average diameter of 24.5mm, and a diametric difference of 0.2mm. G' in this data set shows a positive linear trend and G" shows a 3rd order polynomial trend.

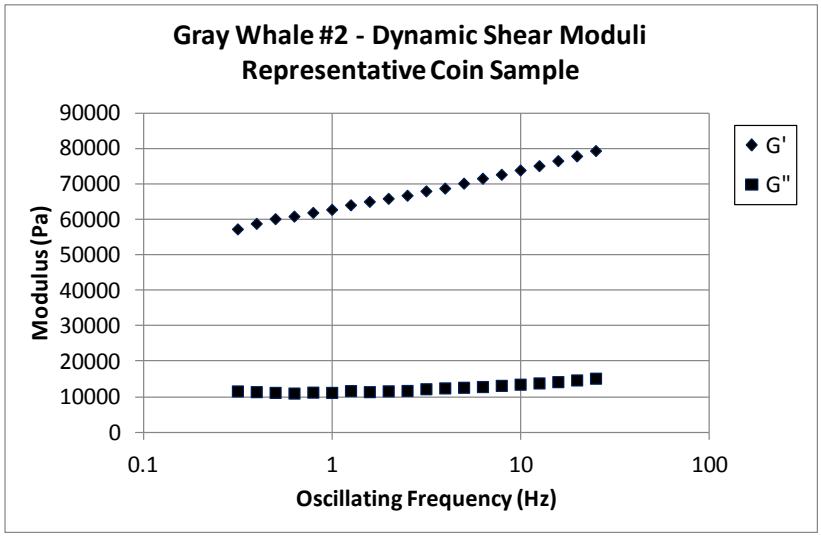

Figure 8: The data set of the representative sample coin for gray whale #2. It shows the value of G' and G" as it changes with the log scale of the oscillating frequency. A conservative estimate for the highest machine measurement error is1500Pa.

Trend lines were fit to the moduli of all of the sample coins for gray whale #2. The coefficient of determination (R^2) of these trend lines were plotted as they varied with depth (Figure 9). Using a log scale for the oscillating frequency, the G' and G" were fit with a linear and 3rd order polynomial respectively. All of the fits showed high agreement with R^2 above 0.870. The vast majority were above R^2=0.960. A polynomial traced through the R^2 data points to define a general depth profile. From this, no large changes were seen (based on scaling).

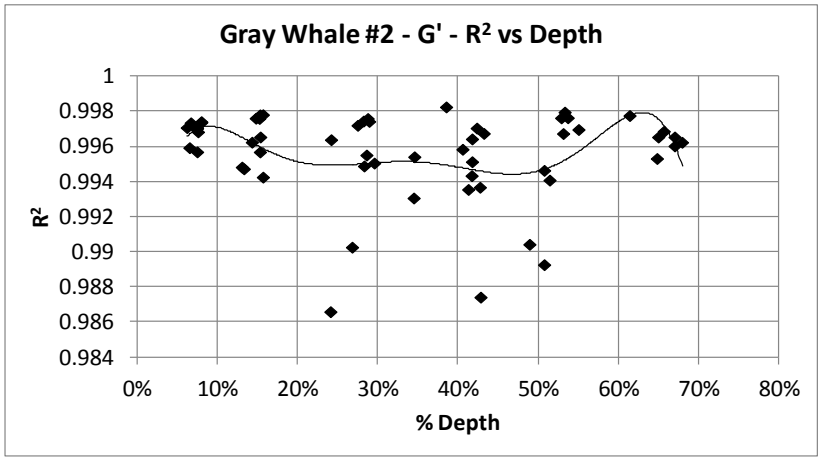

(a)

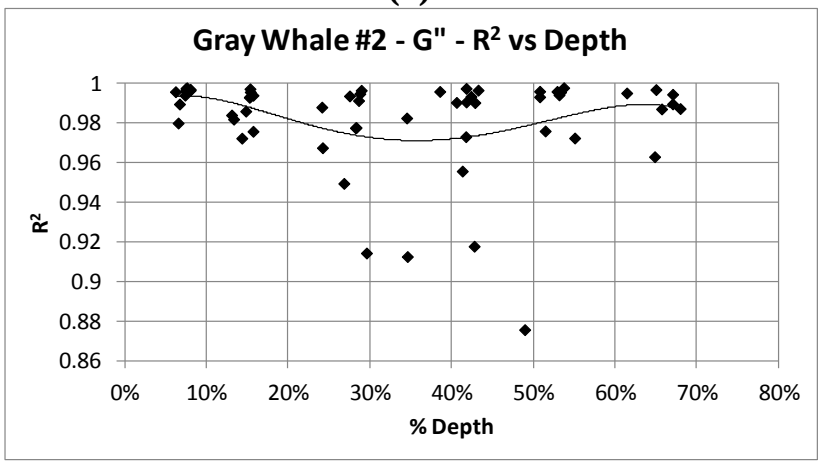

(b)

Figure 9: a) R^2 plotted against depth, for the trend lines of all of the sample coins in gray whale #2: a) G' – linear fit b) G" – 3rd order polynomial fit.

Figure 10 is a series of plots, each showing the general depth profile of a different rheometric property for gray whale #2. In each plot, the 3.1Hz data points from all 58 sample coins are plotted against depth, and a polynomial traces the general depth profile through this data. In addition, polynomials are traced through the 25Hz and 0.31Hz data points. For clarity, the data points for these latter two data sets are not shown. . The shapes of all three depth profiles are similar in each plot. For G' and G", the profiles show a general linear trend between ~19% and ~55% depth. The sections

of the profiles that are shallower and deeper than this middle region show a different behavior. This may be due to a transition in tissue constituents as it gets closer to the dermis and the superficial fascia layer. This profile region separation is less distinct for the G"/G' plot, which shows a slight increase with depth.

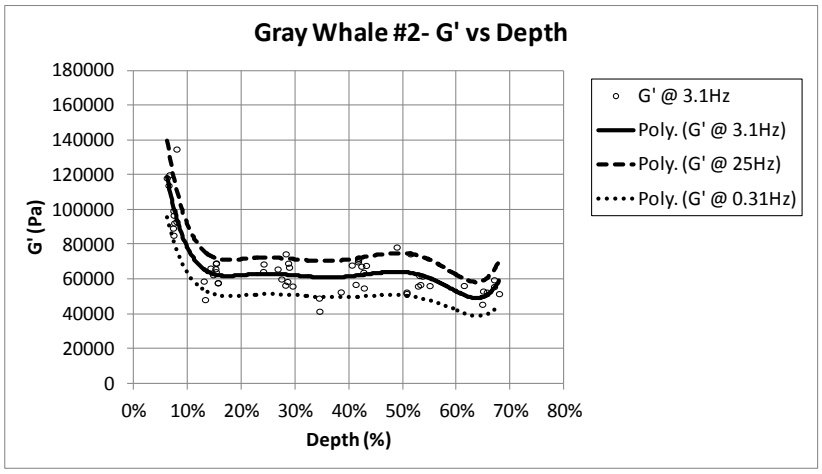

(a)

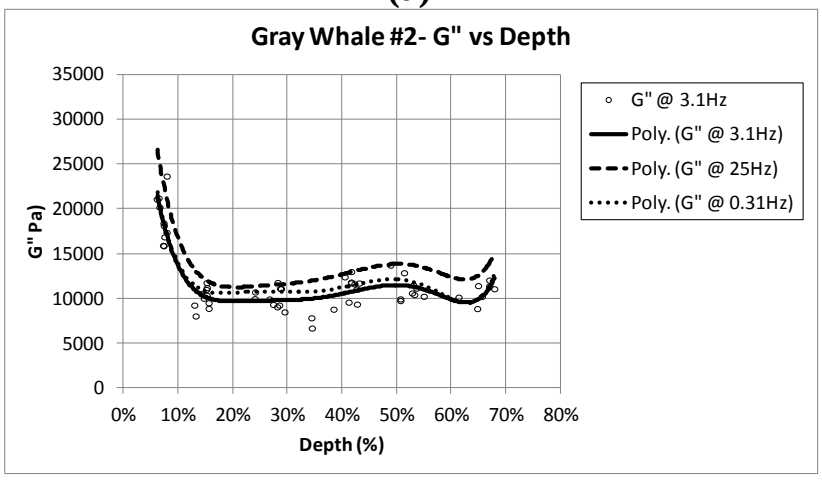

(b)

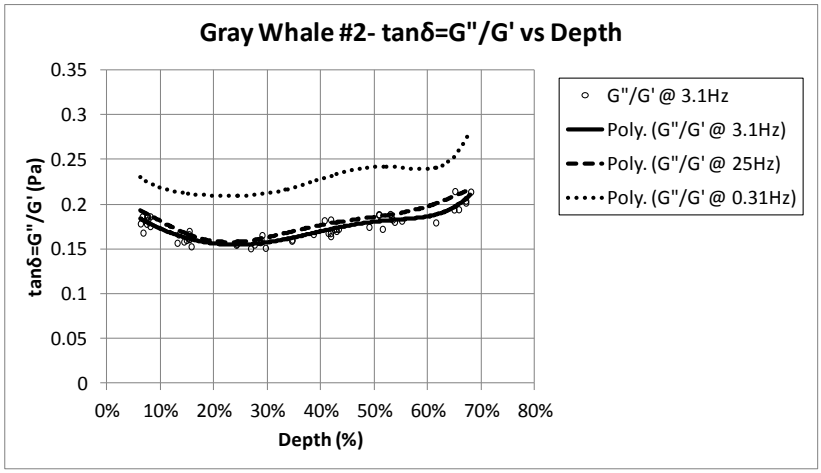

(c)

Figure 10: A series of plots that show rheometric properties as they vary with depth in gray whale #2. Displayed are the data points measured at 3.1Hz and depth profile traces through these data points and the data points of 25Hz and 0.31Hz: a) G' b) G" c) tanδ=G"/G'

3.1.5 Sperm Whale

A blubber sample from a sperm whale was received from Bruce Mate (Director of the Marine Mammal Institute). The sample had been collected and frozen from one of the whales in the mass stranding in 1979, near the mouth of the Siuslaw River in Oregon. Information was not available on the animal's size, age, or gender, but based on the summary of all the animals listed in the mass stranding the length would have been between 9.3m and 11.5m. [7] It was also unknown, where, on the body, the sample was extracted. Not surprisingly, the sample was negatively affected from being frozen for such a long period. The outer exposed surfaces of the block were completely desiccated and very hard. A sub-block cut from the original block shows this intense, slightly translucent orange, damaged tissue (Figure 11). In April 2013 (34 years in storage) the block (89.7-103.4mm thick) was thawed and the desiccated tissue was measured and removed. The soft, encased tissue was prepared and tested as described in the methods section. Ten columns were cut into the block,

all within a 0.3m^2 area. Within these ten columns, 47 sample coins, at various depths, were tested.

Figure 11: Sub-block cut from the original. It shows the desiccated, damaged tissue (orange color) caused by long term freezing.

The geometry of the tested coins was evaluated to see if their variability caused variability in the dynamic shear moduli measurements (Table 4). The variability of most of these values was expected, given the difficulty of cutting soft tissue. Though not large imbalances most of the sample coins nearest to the dermis had the largest diameters, while the deepest samples were the thickest and most elliptical.

Table 4: The range of geometric values measured for the sperm whale sample coins.

Sperm Whale: Coin-Sample Geometries			
	Maximum	Average	Minimum
Thickness (mm)	8.2	4.1	2.9
Diametric Average (mm)	24.5	21.6	19.1
Diametric Difference (mm)	4.8	1.2	0.04

A representative sample coin was selected to show the typical moduli measurements for the sperm whale. Figure 12 plots G' and G" against the log scale of the oscillating frequency. The coin selected was taken from a 57.4% depth in the tissue. It was 3.1mm thick, had an average diameter of 21.6mm, and a diametric

difference of 0.2mm. G' in this data set shows a positive linear trend and G" shows a 3rd order polynomial trend.

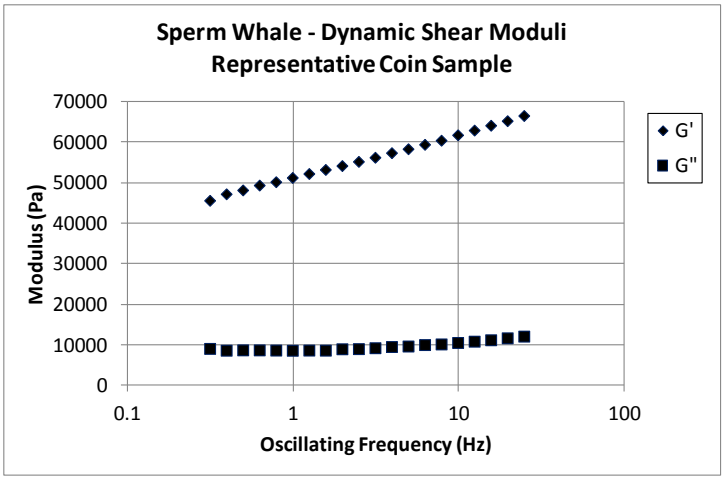

Figure 12: The data set of the representative sample coin for the sperm whale. It shows the value of G' and G" as it changes with the log scale of the oscillating frequency. A conservative estimate for the highest machine measurement error is1500Pa.

Trend lines were fit to the moduli of all of the sample coins for the sperm whale. The coefficient of determination (R^2) of these trend lines were plotted as they varied with depth (Figure 13). Using a log scale for the oscillating frequency, the G' and G" were fit with a linear and 3rd order polynomial respectively. All of the fits showed high agreement with R^2 above 0.991. The vast majority were above R^2=0.994. A polynomial traced through the R^2 data points to define a general depth profile. From this, no large changes were seen (based on scaling).

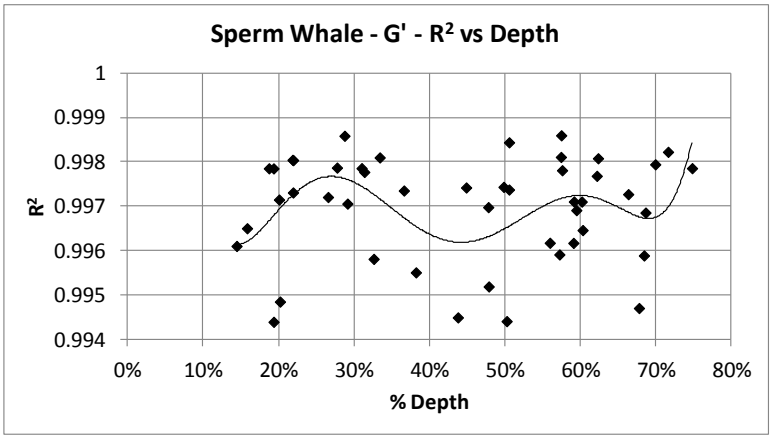

(a)

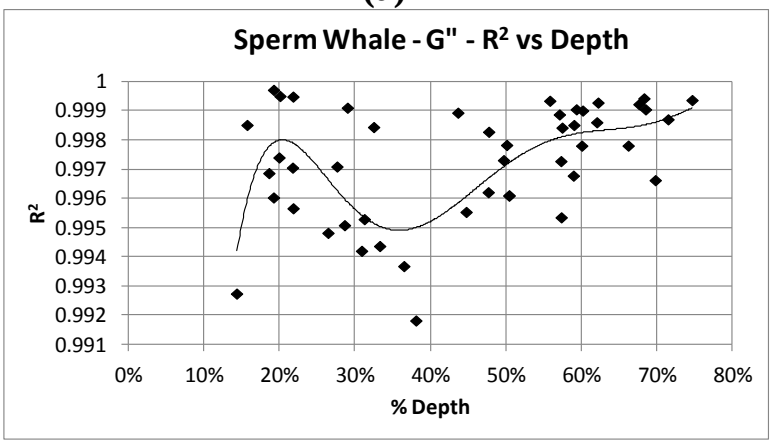

(b)

Figure 13: a) R^2 plotted against depth, for the trend lines of all of the sample coins in the sperm whale: a) G' – linear fit b) G" – 3rd order polynomial fit.

Figure 14 is a series of plots, each showing the general depth profile of a different rheometric property for the sperm whale. In each plot, the 3.1Hz data points from all 47 sample coins are plotted against depth, and a polynomial traces the general depth profile through this data. In addition, polynomials are traced through the 25Hz and 0.31Hz data points. For clarity, the data points for these latter two data sets are not shown. The shapes of all three depth profiles are similar in each plot. For G' and G", the profiles show a general linear trend between ~32% and ~54% depth. The sections

of the profiles that are shallower and deeper than this middle region show a different behavior. This may be due to a transition in tissue constituents as it gets closer to the dermis and the superficial fascia layer. This profile region separation is less distinct for the G"/G' plot, which shows an increase with depth.

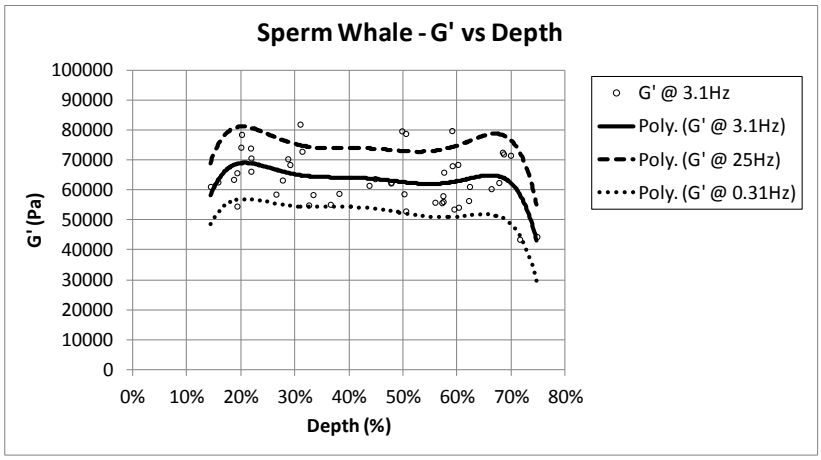

(a)

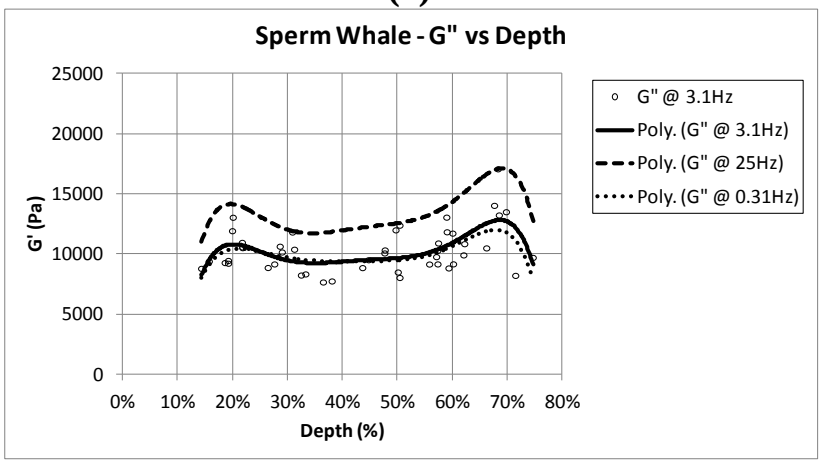

(b)

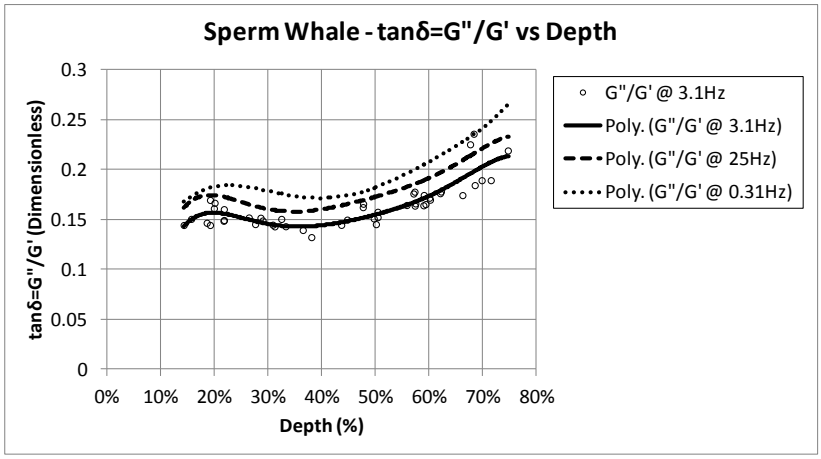

(c)

Figure 14: A series of plots that show rheometric properties as they vary with depth in the sperm whale. Displayed are the data points measured at 3.1Hz and depth profile traces through these data points and the data points of 25Hz and 0.31Hz: a) G' b) G" c) tanδ=G"/G'

3.2 Collagen/Non-Collagen Protein

3.2.1 General Observations

Images were taken at different stages in the staining assay protocol for each whale. Figure 15 shows the tissue sections before and after (backlight) they were stained, and after the stain was extracted. This post extraction photo shows the tissue squares spatially oriented to their locations in the original tissue sections. The width of each square was typically 8.5-11.3mm. The height ranged from 8.1mm to 10.2mm, with a few of the deepest squares being cut short (as low as 5.1mm) to gain additional data points. The coloration of the pre-stained sections was different between species, but similar for the same species (gray whale). This characteristic was less noticeable in the stained photos because the two gray whale samples had different thicknesses so light passed through them differently. Each section showed a consistent depth change in its stain colorations and tissue structures across its width. The slight exception to

this was the sperm whale section. At its deepest tissue depths (near the superficial fascia) there was damaged, desiccated tissue (pale orange color). This is most easily seen in both the stained photo and the extracted photo. This damaged tissue was not able to absorb as much stain as the rest of the section. For all of the sections, there was remnant stain in the tissue, after extraction. More so near the top and bottom of each column. Some of this can be attributed to homogenous discoloration from the tissue squares soaking in their respective extraction buffer / stain solutions. However, it is thought that there is still stain attached to collagen in the more intensely discolored regions (light red hue).

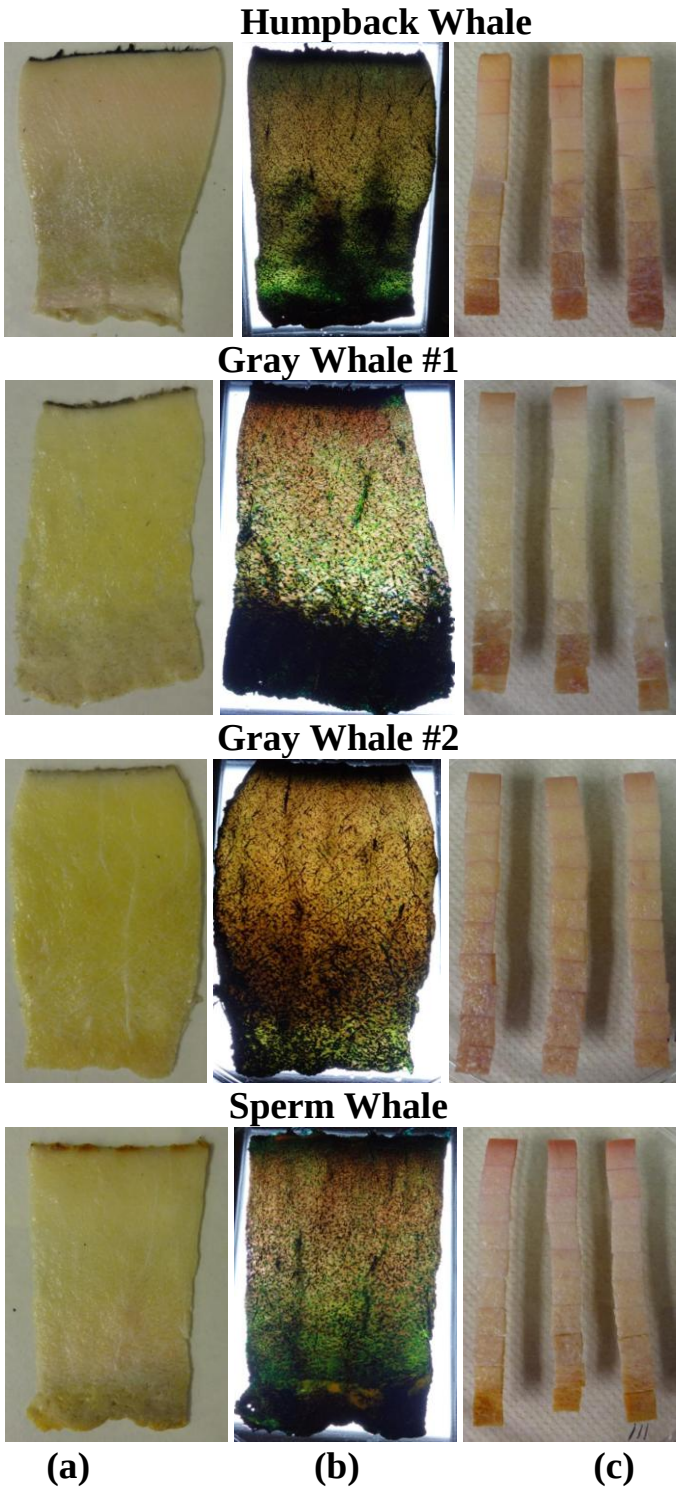

Figure 15: Images at different stages of the staining assay protocol for all four whales. a) Tissue sections before staining (90-110mm long by 50-70mm wide). b) Tissue sections backlight after staining. c) Tissue squares post stain extraction (spatially oriented as they were cut from the original sections).

3.2.2 Humpback Whale

The normalized protein concentrations measured for the humpback whale were plotted to find changes with depth. Polynomial curves were traced through each plot to define a depth profile. Both the amount of collagen (Figure 16a) and non-collagen protein (Figure 16b) in the tissue follow similar profiles, and both increase with depth. In Figure 16c, the ratio of non-collagen to collagen protein has a relatively linear, positively sloped, correlation with depth. This indicates an increase in proportion of non-collagen protein. Lastly, Figure 16d shows that the thicknesses of the squares varied from ~2.5mm-3.5mm, and that the depth profile of thickness does not match the protein profiles.

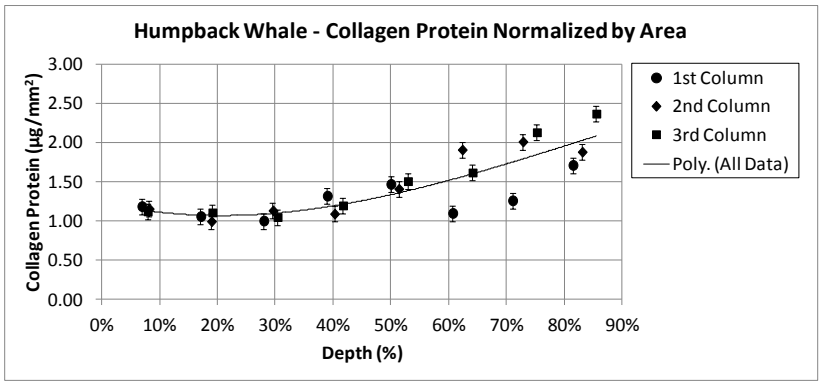

(a)

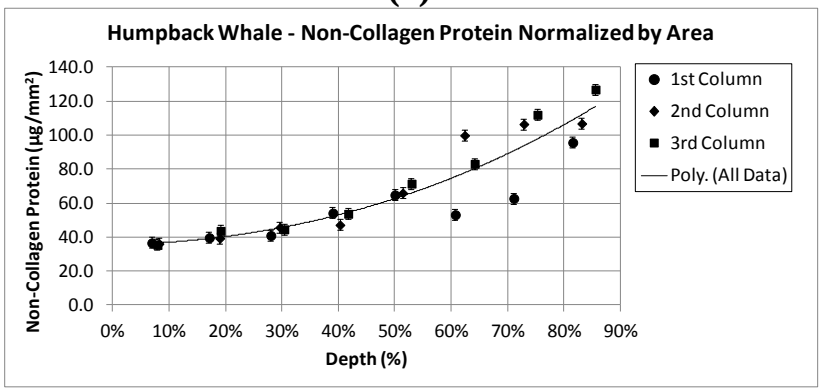

(b)

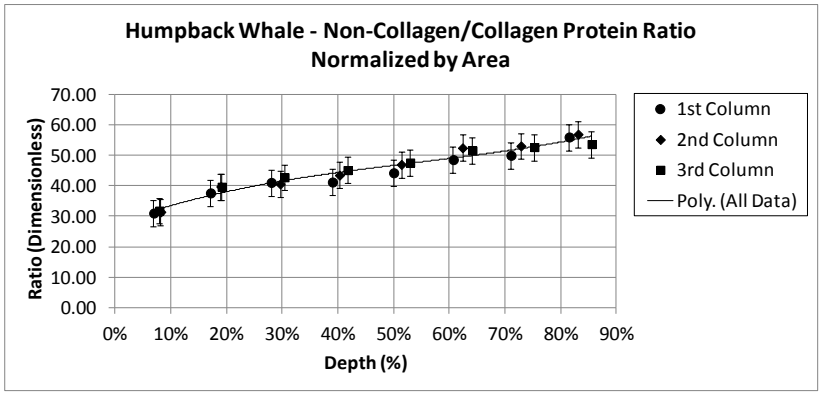

(c)

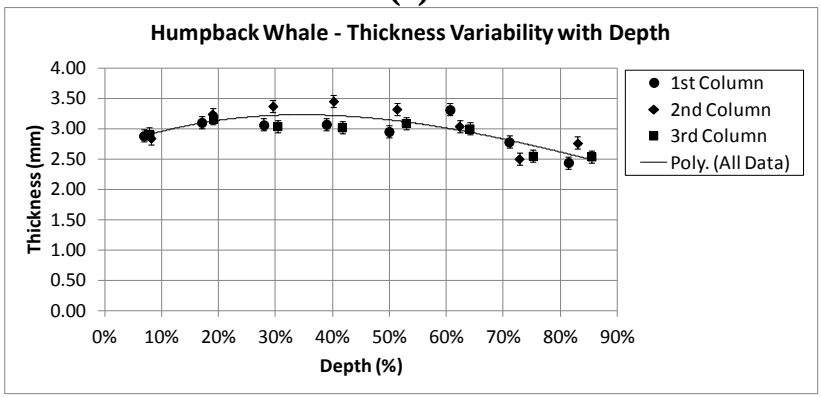

(d)

Figure 16: The measured values from the humpback tissue staining assay plotted against depth. a) Normalized collagen protein concentration. b) Normalized non-collagen protein concentration. c) Ratio of non-collagen to collagen protein concentrations. d) Sample square thickness.

3.2.3 Gray Whale #1

The normalized protein concentrations measured for the gray whale #1 were plotted to find changes with depth. Polynomial curves were traced through each plot to define a depth profile. Both the amount of collagen (Figure 17a) and non-collagen protein (Figure 17b) in the tissue follow similar profiles. They both decrease until ~48% depth and then increase again until ~80% depth making a U-shape. In Figure 17c, the ratio of non-collagen to collagen protein slight decreases until ~30% depth and then increases through ~85% depth. This shows the relative decrease and increase in the proportion of non-collagen protein content. Lastly, Figure 17d shows that the

thicknesses of the squares varied from ~0.8-1.5mm, and that the depth profile of thickness does not match the protein profiles.

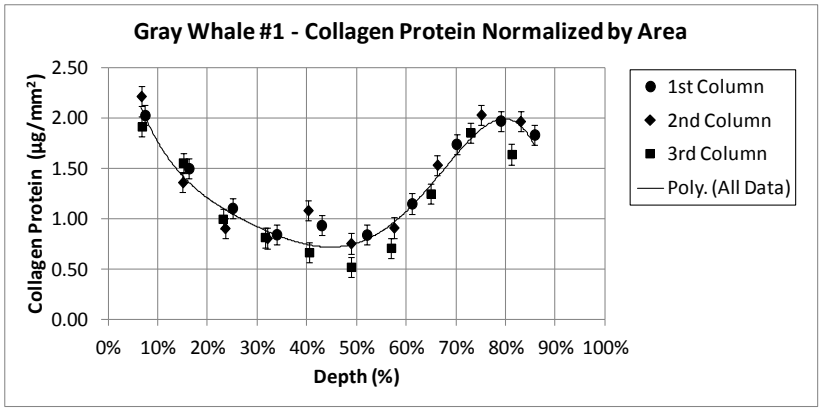

(a)

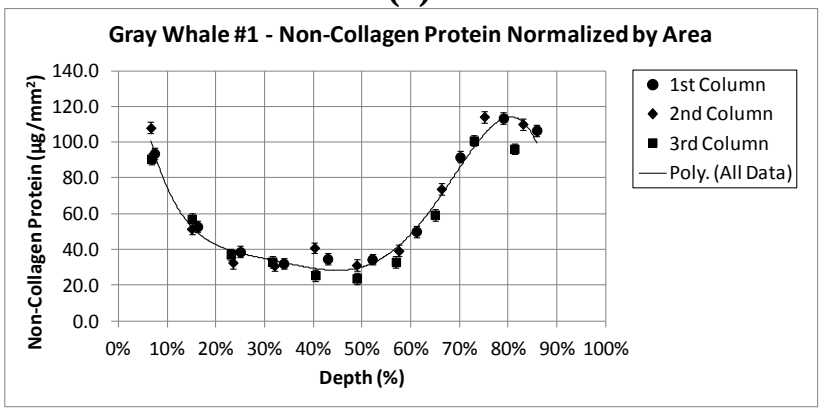

(b)

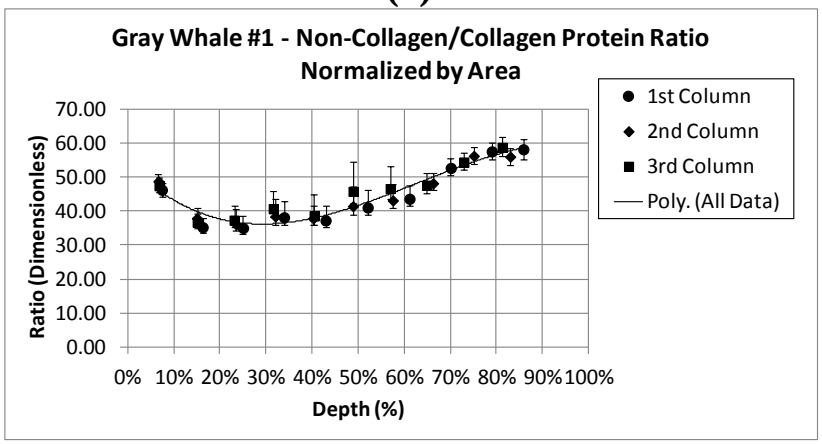

(c)

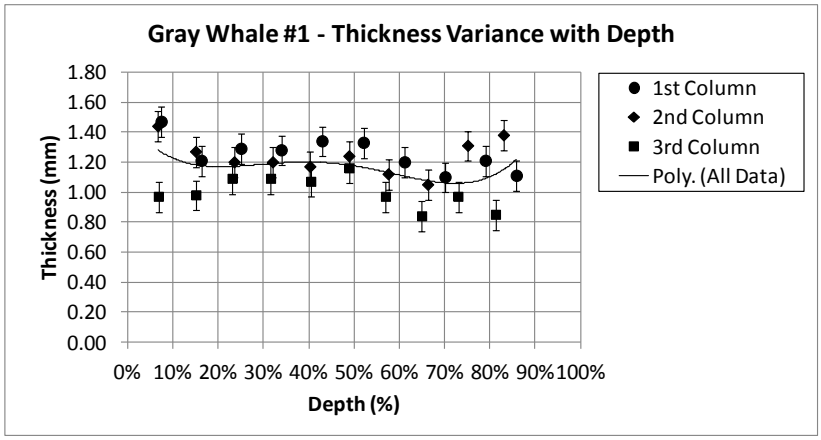

(d)

Figure 17: The measured values from the gray whale #1 tissue staining assay plotted against depth. a) Normalized collagen protein concentration. b) Normalized non-collagen protein concentration. c) Ratio of non-collagen to collagen protein concentrations. d) Sample square thickness.

3.2.4 Gray Whale #2

The normalized protein concentrations measured for the gray whale #2 were plotted to find changes with depth. Polynomial curves were traced through each plot to define a depth profile. Both the amount of collagen (Figure 18a) and non-collagen protein (Figure 18b) in the tissue follow similar profiles. They both decrease until a depth of ~33% and then slightly increase through a depth of ~80%. In Figure 18c, the ratio of non-collagen to collagen protein very slightly decreases until ~30% depth and then follows a relatively linear, positively sloped, correlation with depth through ~86% depth. This shows the relative decrease and increase in the proportion of non-collagen protein content. Lastly, Figure 18d shows that the thicknesses of the squares varied from ~2.0mm-3.2mm, and that the depth profile of thickness does not match the protein profiles.

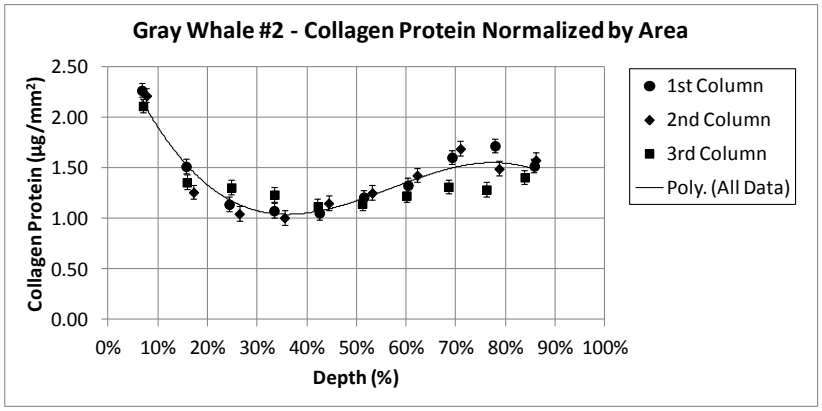
Gray Whale #2 - Collagen Protein Normalized by Area
Collagen Protein (µg/mm²)
2.50
2.00
1.50
1.00
0.50
0.00
0% 10% 20% 30% 40% 50% 60% 70% 80% 90% 100%
Depth (%)
1st Column
2nd Column
3rd Column
Poly. (All Data)

(a)

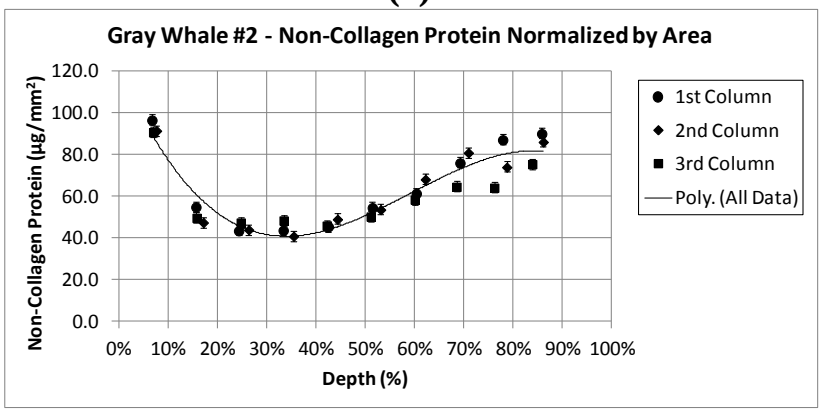
Gray Whale #2 - Non-Collagen Protein Normalized by Area
Non-Collagen Protein (µg/mm²)
120.0
100.0
80.0
60.0
40.0
20.0
0.0
0% 10% 20% 30% 40% 50% 60% 70% 80% 90% 100%
Depth (%)
1st Column
2nd Column
3rd Column
Poly. (All Data)

(b)

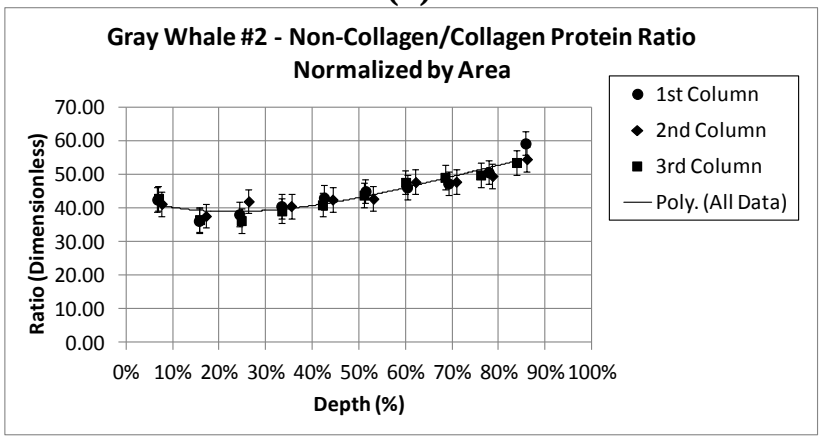
Gray Whale #2 - Non-Collagen/Collagen Protein Ratio Normalized by Area
Ratio (Dimensionless)
70.00
60.00
50.00
40.00
30.00
20.00
10.00
0.00
0% 10% 20% 30% 40% 50% 60% 70% 80% 90% 100%
Depth (%)
1st Column
2nd Column
3rd Column
Poly. (All Data)

(c)

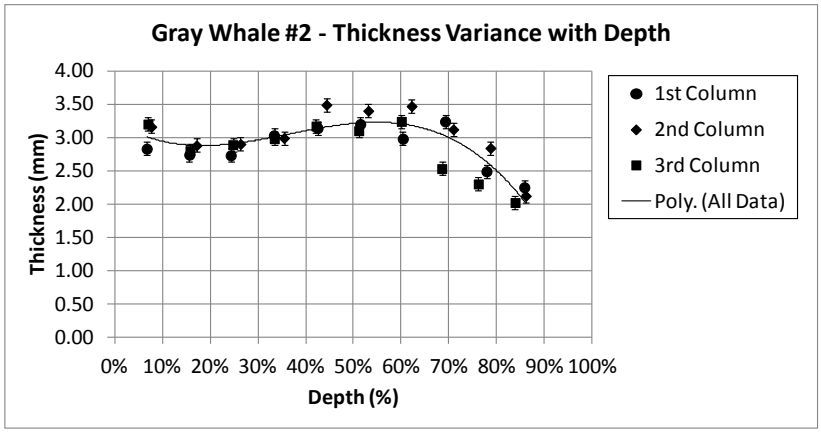

(d)

Figure 18: The measured values from the gray whale #2 tissue staining assay plotted against depth. a) Normalized collagen protein concentration. b) Normalized non-collagen protein concentration. c) Ratio of non-collagen to collagen protein concentrations. d) Sample square thickness.

3.2.5 Sperm Whale

The normalized protein concentrations measured for the sperm whale were plotted to find changes with depth. Polynomial curves were traced through each plot to define a depth profile. Both the amount of collagen (Figure 19a) and non-collagen protein (Figure 19b) in the tissue follow similar profiles. They both decrease and level off between ~25% and ~60% depth, and then continue to decrease through ~84% depth. In Figure 19c, the ratio of non-collagen to collagen protein remains relatively constant with slight rise from ~7% to ~85% depth. This indicates an increase in proportion of non-collagen protein. Lastly, Figure 19d shows that the thicknesses of the squares varied from ~2.0mm-3.5mm, and that the depth profile of thickness does not match the protein profiles. It should be noted that the decrease in protein content between ~60% and ~85% may be attributed to less absorbed stain in these damaged and desiccated sample squares.

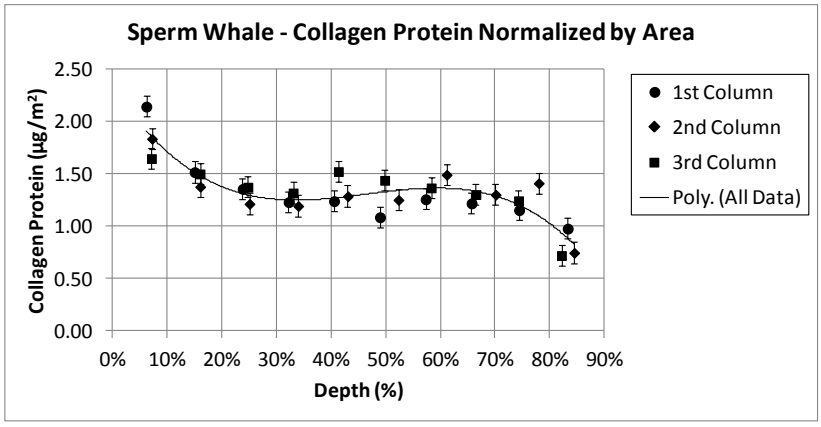
Sperm Whale - Collagen Protein Normalized by Area
Collagen Protein (µg/m²)
2.50
2.00
1.50
1.00
0.50
0.00
0%
10%
20%
30%
40%
50%
60%
70%
80%
90%
Depth (%)
1st Column
2nd Column
3rd Column
Poly. (All Data)

(a)

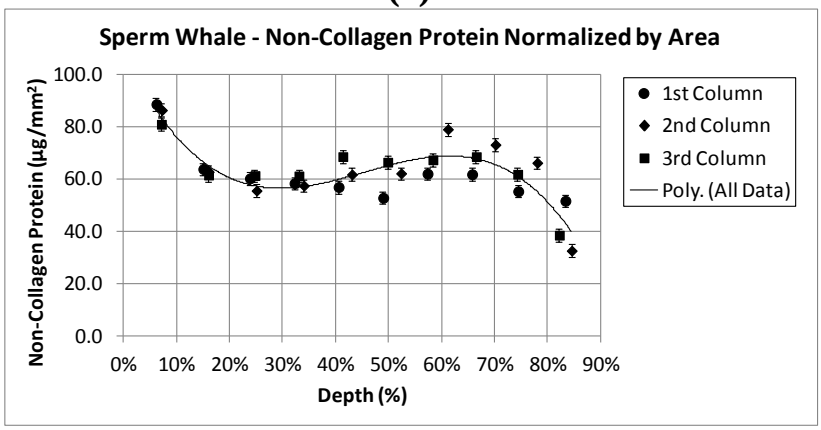
Sperm Whale - Non-Collagen Protein Normalized by Area
Non-Collagen Protein (µg/mm²)
100.0
80.0
60.0
40.0
20.0
0.0
0%
10%
20%
30%
40%
50%
60%
70%
80%
90%
Depth (%)
1st Column
2nd Column
3rd Column
Poly. (All Data)

(b)

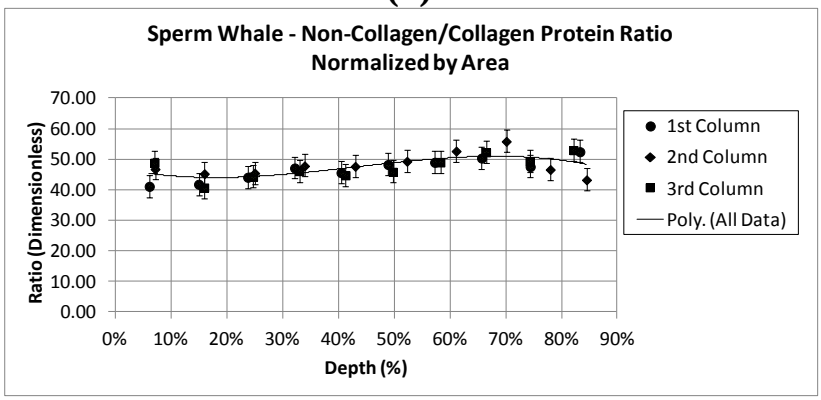
Sperm Whale - Non-Collagen/Collagen Protein Ratio
Normalized by Area
Ratio (Dimensionless)
70.00
60.00
50.00
40.00
30.00
20.00
10.00
0.00
0%
10%
20%
30%
40%
50%
60%
70%
80%
90%
Depth (%)
1st Column
2nd Column
3rd Column
Poly. (All Data)

(c)

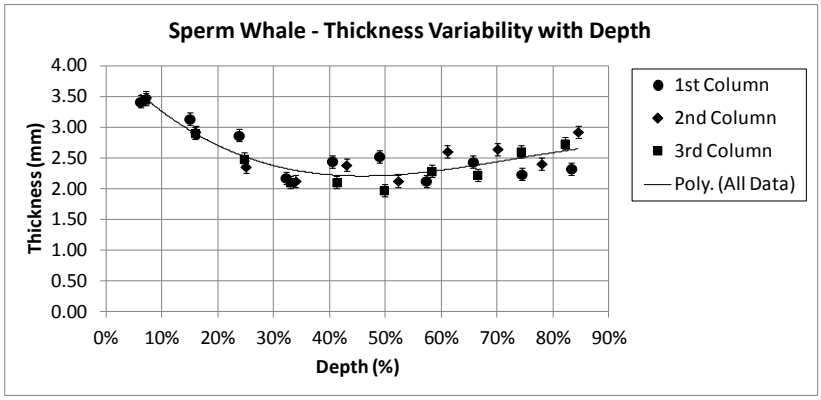

(d)

Figure 19: The measured values from the sperm whale tissue staining assay plotted against depth. a) Normalized collagen protein concentration. b) Normalized non-collagen protein concentration. c) Ratio of non-collagen to collagen protein concentrations. d) Sample square thickness.

4 Discussion

4.1 Strain Sweep

The strain sweep data was checked for linearity. Coins were selected out of a single column for each whale, with exception to the humpback whale, which was not tested in this way. Gray whale #1 was tested at 9.8%, 20%, 36%, 50%, and 62% depth, and measured seven data points across the sweep of 0.1-2% strain. Gray whale #2 was tested at 7.6%, 15%, 29%, 42%, 53%, and 67% depth, and measured 17 data points across the sweep of 0.1-2% strain. And lastly, the sperm whale was tested at 19%, 28%, 45%, 58%, and 62% depth, and measured 33 data points across the sweep of 0.1-2% strain. The resulting plots show a linear relationship between the percent strain and the measured G' values at both 1Hz and 10Hz, when evaluated near 1% strain. Two strain sweep tests were rejected based on the normal force not remaining constant at 40N throughout the sweep (gray whale #1, 1Hz, at 9.8% and 20% depth). However,

based on the linearity these samples still showed and the consistency in linearity for the rest of the data sets, it is assumed that, had the load been maintained, these samples would have shown the same response.

4.2 Repeat Frequency Sweep

The repeat frequency sweep data was analyzed for rheometric measurement repeatability. Coins were selected for testing from a single column for each whale. The humpback whale was tested at 5.4% depth. Gray whale #1 was tested at 9.6%, 19.7%, 34.5%, 49.1%, and 61.1% depth. Gray whale #2 was tested at 7.5%, 15.4%, 28.8%, 55.1%, and 65.7% depth. And lastly, the sperm whale was tested at 18.7%, 26.5%, 55.9%, and 60.2% depth. The difference in G' and G" values was evaluated at 3.1Hz for these tests. The humpback whale, gray whale #2 and the sperm whale have very similar results. Taken as a whole, their range of G' and G" differences is -5.2% to 2.0% and -3.1% to 5.1%, respectively. These small ranges of measurement repeatability can be attributed to the precision of the rheometer and the loss of fluid observed during testing. The results from gray whale #1 are very different from the other three. Its range of percent change for G' is 11% to 28% and for G", 3% to 29%. From the data collected it is unclear why this disparity occurred. It is highly unlikely that gray whale #2 would show more similarity with two whales of different species than with one of its own. Thus, it is thought that some unknown error occurred during the testing of gray whale #1, and that it should be considered an outlier.

4.3 Dynamic Shear Moduli

The dynamic shear moduli were compared between the whales, at 3.1Hz. Each species has different G' (Figure 20a) and G" (Figure 20b) depth profile characteristics; the two gray whales showed some similarity. This implies that species have specific depth profiles and that the ones shown in this study are not random. However, the freezer storage length is the most similar between the gray whales, and the sperm whale not only was frozen a very long time, but showed a large degree of freezer damage. This may have caused the deviation in shape at the shallower and deeper depths. In addition, the humpback whale shows a much higher elasticity. This may be explained by the fact that its samples were taken in proximity to the ventral grooves, which have a highly elastic tissue structure. In other words, if the frozen storage time cannot be ruled out as affecting the measurements of coins near the dermis and superficial fascia layer, it may be shown that there is not a significant difference between the species; the differences seen may be primarily based on the function of the blubber itself and its location on the whale. Each of the profiles for the rheometric properties (G', G", and G"/G') has similar orders of magnitude between the whales, which implies that the basic structural elements and compositions of blubber are similar across species. When considering the G"/G' (Figure 20c) depth profiles it can be seen that all four whales show a positive shift in the proportion of G" with increased depth. Additionally, these profiles are similar in magnitude. The gray whale depth profiles are the most similar. Their similarities along with their differences to the sperm whale and humpback whale profiles further supports that different species

have distinctly different dynamic shear moduli characteristics. However, more data is needed from additional strandings to support this. From the geometric information gathered, and notation of the geometric imbalances at certain depths for certain coin samples, there is no clear correlated effect of geometry on the measured values of G' or G".

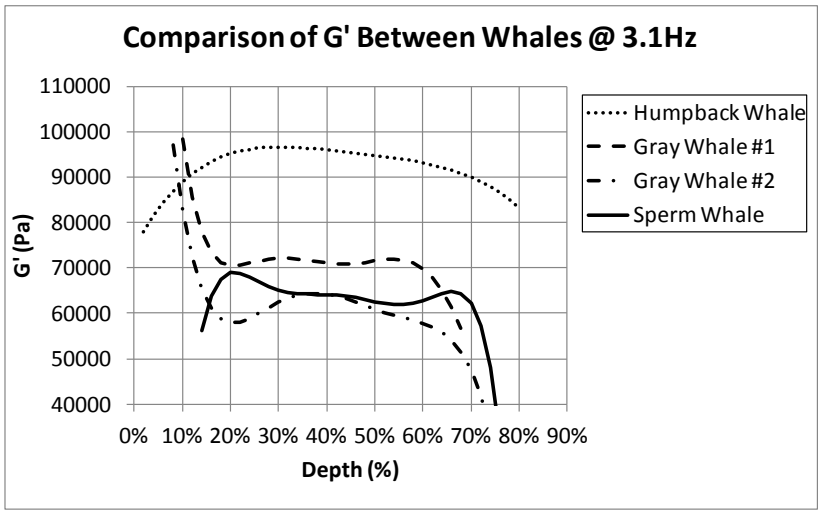

(a)

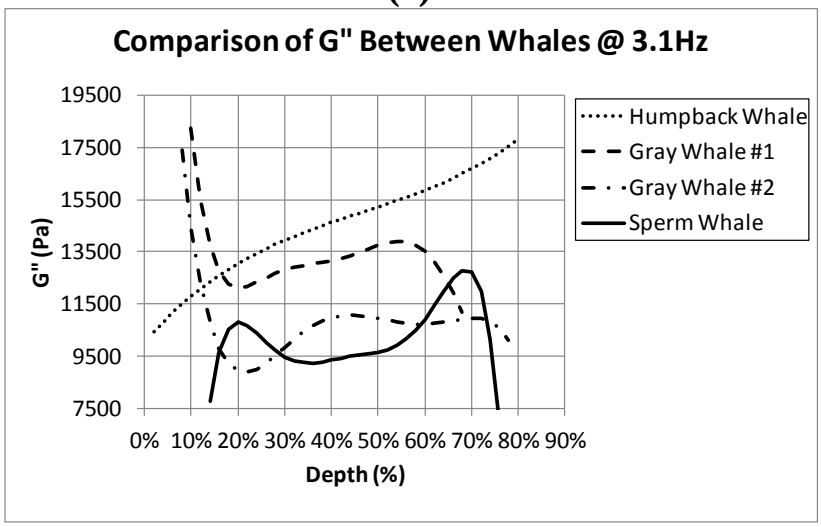

(b)

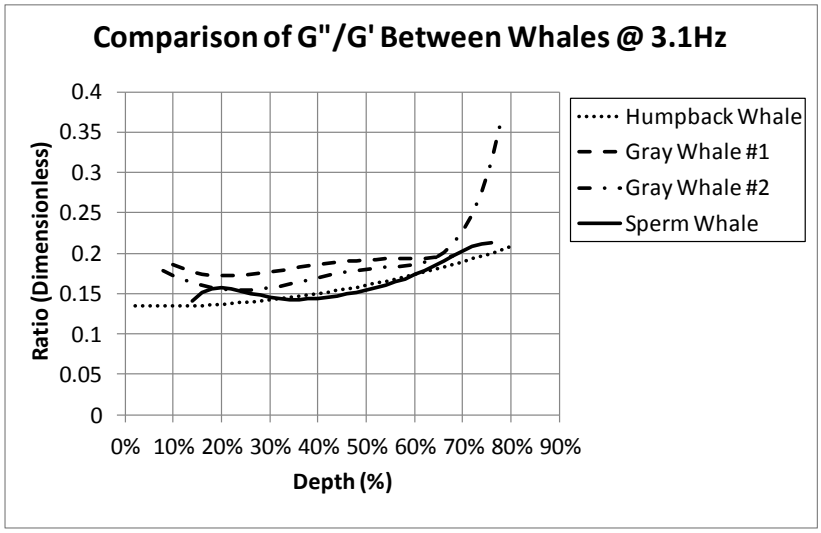

(c)

Figure 20: A comparison of the dynamic shear moduli components between the tested whales, at 3.1Hz, as a function of blubber depth.

The dynamic shear moduli of the pilot whale, calculated from the dynamic shear compliance measured by Fitzgerald and Fitzgerald, was compared to the whales in this study, at 25Hz. Their measurements were performed on a 3.05m long, 340kg female pilot whale. Their blubber sample was extracted from the whale's side, 101.6mm down from the dorsal fin. The extraction depth was 12.7mm. The average length, weight, and blubber thickness of female pilot whales is estimated to be 3.66m, 998-1180kg, and 18-21mm. Since it is unknown how the female's size (being smaller than average) affected her blubber thickness, which was not explicitly defined by Fitzgerald and Fitzgerald, the range of depths assumed for their measured values of G' and G" would have been in the 50-80% depth range. The comparison shows that for both G' (Figure 21a) and G" (Figure 21b), the pilot whale shares a similar order of magnitude to the other whales. However, the G"/G' ratio (Figure 21c) of the pilot whale was significantly lower than the others. Without measured values of the tissue

constituents it isn't possible to deduce why this ratio is so different. However, this comparison still supports that different species have different characteristics, while remaining similar in magnitude.

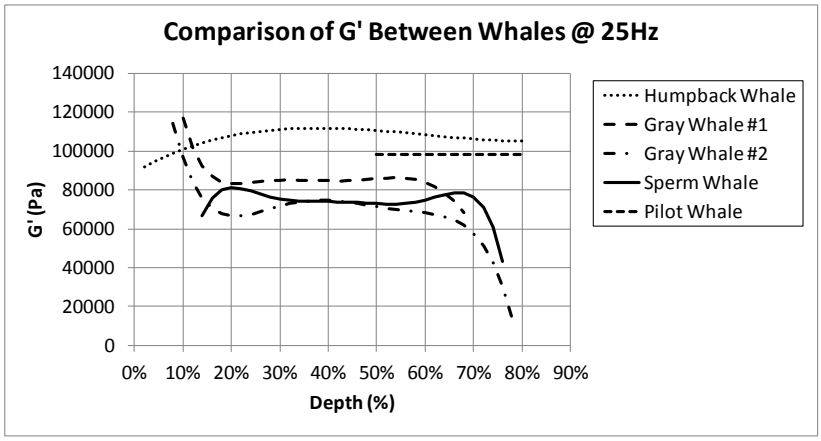

(a)

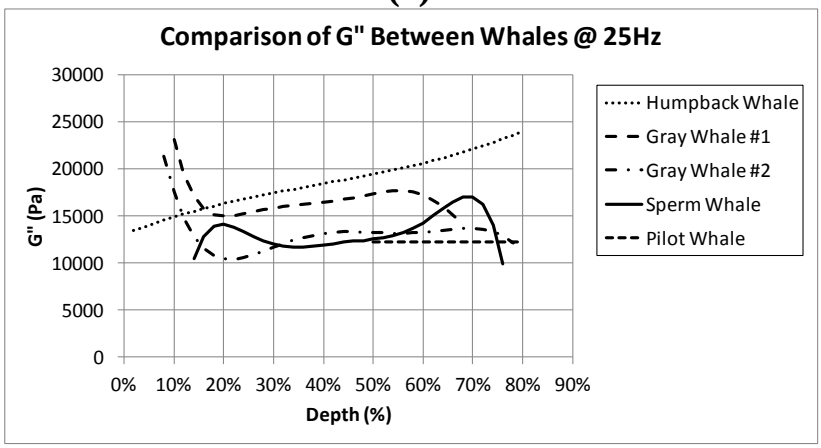

(b)

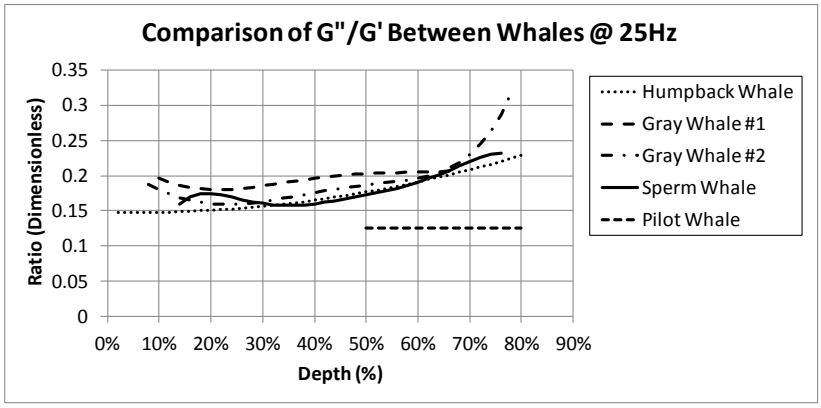

(c)

Figure 21: A comparison of the dynamic shear moduli components between the tested whales and the pilot whale (measured by Fitzgerald and Fitzgerald), at 25Hz, as a function of blubber depth.

4.4 Collagen/Non-Collagen Protein

The collagen and non-collagen protein content were compared between the whales (Figure 22). Since each was normalized, their values were only used for relative comparison to how collagen and non-collagen proteins changed with depth. As was the case for the dynamic shear moduli profiles, the orders of magnitude of the depth profiles for both protein types are similar for all of the whales. Further, the characteristics of the profiles were more similar between the gray whales than between the other species. The only similarity between the dynamic shear component profiles and the protein profiles was between their ratios (non-collagen/collagen and G”/G’). Both show a general increase with depth. This suggests that as the proportion of non-collagen protein increases the tissue responds with a lower storage modulus. This follows the original observation that the deeper coin samples felt less stiff.

The thicknesses of the square samples were compared to determine if normalizing by cross-sectional area was appropriate (Figure 22d). As stated in the results section, there was no clear connection between the shape profiles of the sample

thickness and the protein profiles. In addition, the samples for gray whale #2 were ~2-3 times thicker than the samples for gray whale #1 and no effective shift was seen in the protein profiles. Thus, the normalization by area is considered valid.

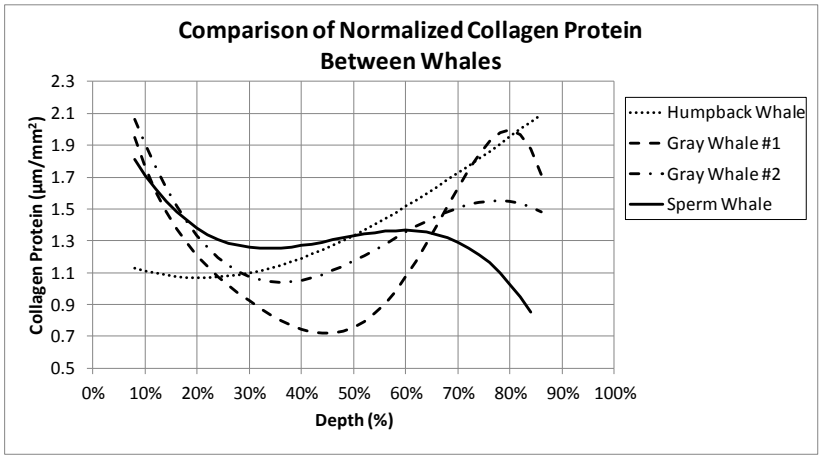

(a)

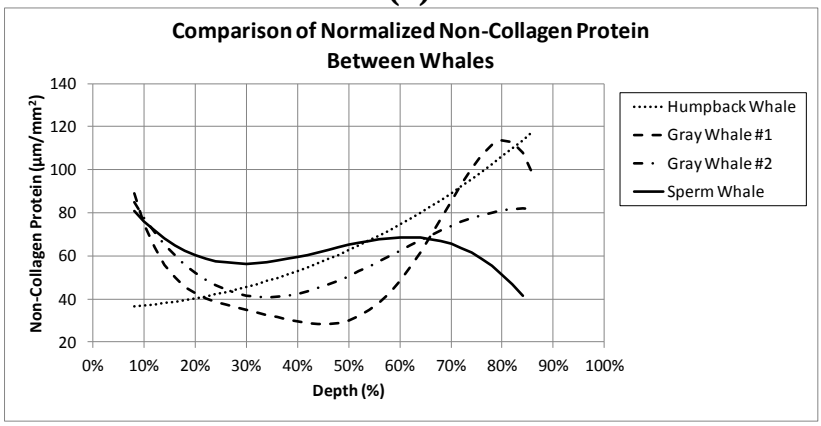

(b)

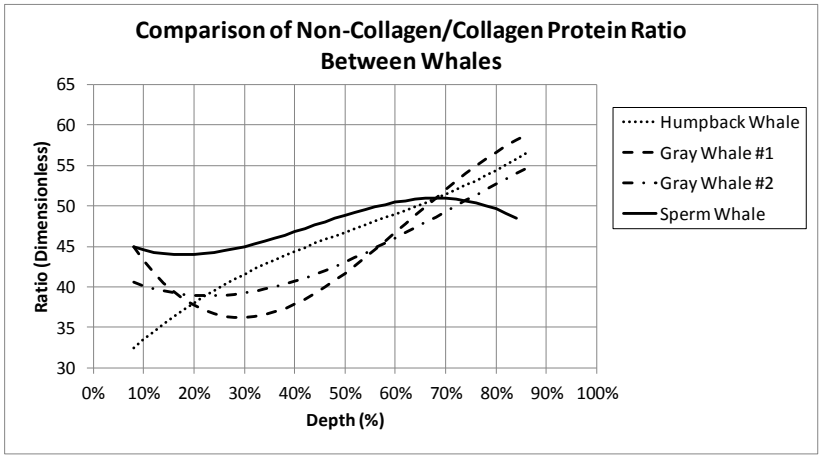

(c)

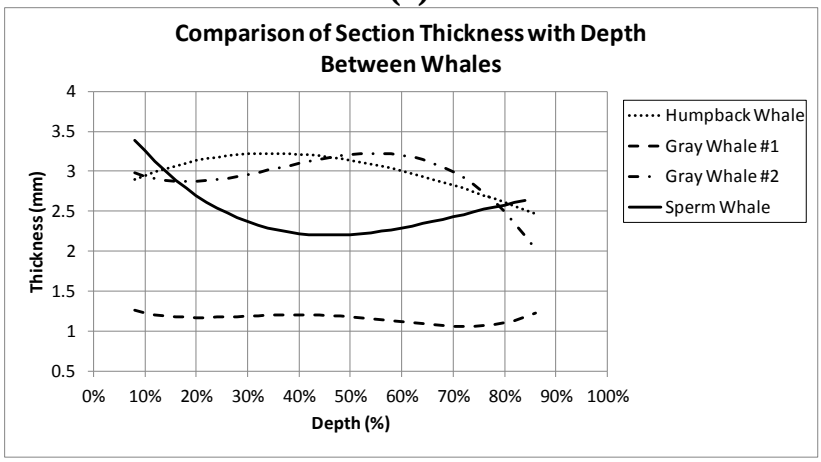

(d)

Figure 22: A comparison of the relative collagen and non-collagen protein content and sample square thickness between the tested whales, as a function of blubber depth.

5 Conclusion

The dynamic shear moduli (G' and G") and relative change in protein content with depth were measured from the blubber of four whales of three different species. The dynamic shear moduli was measured across a range of frequencies (0.31-25Hz), and both the collagen and non-collagen protein content were normalized by cross-sectional area.

The results showed that different whale species may have distinctly different depth profiles of G', G", collagen protein, and non-collagen protein, but also show a similarity in the orders of magnitude of these metrics. A potential correlation exists between the ratios of non-collagen/collagen protein and G"/G'. However, no direct relation was found between the moduli and changes in the individual protein contents.

Future research should be conducted to add to the data in this study. Tests conducted on additional whales, age ranges, and seasonal nutrition levels will begin to fully define the dynamic shear moduli of a whale's blubber throughout its life cycle. This is important for applications such as tagging, where whales at different stages in their life cycle may need to be considered. In addition to the tests outlined in this study, measurements of other tissue constituents (lipids, water content, etc.) should also be performed in order to find additional correlations to the dynamic shear moduli. If such a connection can be made, there is a potential that the dynamic shear moduli of whales from past studies could be estimated from these tissue constituents with minimal effort.

6 Bibliography

[1] D. Reeb, P. B. Best, and S. H. Kidson, “Structure of the integument of southern right whales, Eubalaena australis,” Anat. Rec.-Adv. Integr. Anat. Evol. Biol., vol. 290, no. 6, pp. 596–613, Jun. 2007.

[2] Y. Fung, Biomechanics: {M}echanical {P}roperties of {L}iving {T}issues. Springer-Verlag, 1993.

[3] B. Mate, R. Mesecar, and B. Lagerquist, “The evolution of satellite-monitored radio tags for large whales: One laboratory’s experience,” Deep-Sea Res. Part Ii-Top. Stud. Ocean., vol. 54, no. 3–4, pp. 224–247, 2007.

[4] L. S. Orton and P. F. Brodie, “Engulfing mechanics of fin whales,” Can. J. Zool., vol. 65, no. 12, pp. 2898–2907, Dec. 1987.

[5] E. Fitzgerald and J. Fitzgerald, “Blubber and Compliant Coatings for Drag Reduction in Water .1. Viscoelastic Properties of Blubber and Compliant Coating Materials,” Mater. Sci. Eng. C-Biomim. Mater. Sensors Syst., vol. 2, no. 4, pp. 209–214, Sep. 1995.

[6] Chondrex Inc., “Sirius Red / Fast Green Collagen Staining Kit.” 2013.

[7] D. W. Rice, A. A. Wolman, B. R. Mate, and J. T. Harvey, “A mass stranding of sperm whales in Oregon: Sex and age composition of the school,” Mar. Mammal Sci., vol. 2, no. 1, pp. 64–69, 1986.